Mobility and transformation of CdSe/ZnS quantum dots in soil: Role of the capping ligands and ageing effect

Andrea Carboni, Alexandre Gélabert, Gaëlle Charron, Stéphane Faucher, Gaetane Lespes, Yann Sivry, Marc F. Benedetti

Mobility and Transformation of CdSe/ZnS Quantum Dots in Soil: Role of the Capping Ligands and Ageing Effect

A. Carboni[1,2]*, A. Gelabert[1], G. Charron[3], S. Faucher[4], G. Lespes[4], Y. Sivry[1] and M. F. Benedetti[1]

[1]Université de Paris, Institut de Physique du Globe de Paris UMR 7154. CNRS, F-75005 Paris, France

[2]Centre de Recherche et d'Enseignement de Géosciences de l'Environnement. Technopole Environnement Arbois-Mediterranee, BP80, 13545 Aix-en-Provence Cedex 04, Aix-en-Provence, France

[3]Laboratoire Matière et Systèmes Complexes (MSC), Univ. Paris Diderot, 75013 Paris, France

[4]Université de Pau et des Pays de l'Adour, CNRS, Institut des Sciences Analytiques et de Physico Chimie pour l'Environnement et les Matériaux (IPREM), UMR 5254, Helioparc, 2 Avenue Pierre Angot, 64053 Pau, France

* Corresponding author

Carboni Andrea

carboni@cerege.fr

Centre de Recherche et d'Enseignement de Géosciences de l'Environnement. TechnopoleEnvironnement Arbois-Mediterranee, BP80, 13545 Aix-en-Provence Cedex 04, Aix-en-Provence, France

Mobility and Transformation of CdSe/ZnS Quantum Dots in Soil: Role of the Capping Ligands and Ageing Effect

A. Carboni[1,2]*, A. Gelabert[1], G. Charron[3], S. Faucher[4], G. Lespes[4], Y. Sivry[1] and M. F. Benedetti[1]

[1]Université de Paris, Institut de Physique du Globe de Paris UMR 7154. CNRS, F-75005 Paris, France

[2]Centre de Recherche et d'Enseignement de Géosciences de l'Environnement. Technopole Environnement Arbois-Mediterranee, BP80, 13545 Aix-en-Provence Cedex 04, Aix-en-Provence, France

[3]Laboratoire Matière et Systèmes Complexes (MSC), Univ. Paris Diderot, 75013 Paris, France

[4]Université de Pau et des Pays de l'Adour, CNRS, Institut des Sciences Analytiques et de Physico Chimie pour l'Environnement et les Matériaux (IPREM), UMR 5254, Helioparc, 2 Avenue Pierre Angot, 64053 Pau, France

* Corresponding author

Carboni Andrea

carboni@cerege.fr

Centre de Recherche et d'Enseignement de Géosciences de l'Environnement. TechnopoleEnvironnement Arbois-Mediterranee, BP80, 13545 Aix-en-Provence Cedex 04, Aix-en-Provence, France

Abstract

The increasing application of Quantum Dots (QDs) is cause of concern for the potential negative effects for the ecosystem, especially in soils that may act as a sink. In this study, soil leaching experiments were performed in quartz sand packed columns to investigate the behavior of core-shell CdSe/ZnS QDs coated with either small ligands (TGA-QDs) or more complex polymers (POAMA-QDs). Fluorescence emission was compared to mass spectrometric measurements to assess the nanoparticles (NPs) state in both the leachate (transported species) and porous media (deposited amounts). Although both QDs were strongly retained in the column, large differences were observed depending on their capping ligand stability. Specifically, for TGA-QDs elution was negligible and the retained fraction accumulated in the top-columns. Furthermore, 74% of the NPs were degraded and 38% of the Se was found in the leachate in non-NPs state. Conversely, POAMA-QDs were recovered to a larger extent (78.1%), and displayed a higher transport along the soil profile. Further experiments with altered NPs showed that homo-aggregation of the QDs prior injection determined a reduced mobility but no significant changes in their stability. Eventually, ageing of the NPs in the column (15 days) caused the disruption of up to 92% of the original QDs and the immobilization of NPs and metals. These results indicate that QDs will accumulate in top-soils, where transformations phenomena will determine the overall transport, persistency and degradation of these chemicals. Once accumulated, they may act as a source for potentially toxic Cd and Se metal species displaying enhanced mobility.

Keywords

Nanoparticles

Quantum dots

Transformation

Mobility

Soil

1. Introduction

Engineered nanoparticles (NPs) are currently incorporated in a large number of consumer products and their production is expected to increase dramatically in the next years (Roco 2011). Quantum Dots (QDs) are among the most promising materials in emerging nanotechnologies due to the unique high-yield and size-tunable electrical and optical properties (Bruchez et al., 1998, Bera et al., 2010), which make them ideal candidates for applications in photovoltaics and biomedical imaging as well as in the construction of sensors and electronics in general (Alivisatos 2004; Kamat 2008; Anikeeva et al., 2009; Kalita et al., 2016). Such properties are correlated to QDs distinctive structure where a semi-conductive metal core, usually composed of CdTe, CdSe or InP, is surrounded by a shell (e.g. ZnS, CdSe). The resulting core-shell nanocrystals have diameters in the 2-100 nm size range and are commonly functionalized with organic polymer coatings in order to increase their stability and solubility in aqueous media, i.e. their applicability (Dabbousi et al., 1997; Bruchez et al., 1998; Bera et al., 2010; Karakoti et al., 2015). There is concern for the possible negative effects arising from the wide usage of engineered nanomaterials and in the last two decades several countries and organizations (e.g. European Commission; US Environmental Protection Agency) have launched campaigns for the study of the associated risks for humans and the ecosystem (Dunphy et al., 2006. Owen et al., 2007; U.S. EPA, 2011; Oomen et al., 2018). In particular, QDs may display peculiar reactivity and persistency and their toxicity could be related to the NPs form, the release of potentially toxic metals and enhanced by the organic ligands (Hardman, 2006) as highlighted by recent works showing the noxious effects on bacteria and eukariota (e.g. Khare and Kumari, 2017). QDs release in the environment can occur from point and diffuse sources, such as the use and disposal of consumer and biomedical products but also the waste production and land application of

91 biosolids. Thus, soil may act as a sink for NPs accumulation and understanding their behavior in the
92 terrestrial ecosystems is of utmost importance for risk assessment and management (Cornelis et al.,
93 2014). However, most research on QDs fate in environmental systems has been focused on
94 freshwater (Xiao et al., 2016) and the number of studies addressing their behavior in other
95 compartments is still limited. Research has been conducted to investigate the deposition of QDs onto
96 porous media employing quartz crystal microbalance (QCM; Quevedo & Tufenkij, 2009; Quevedo et
97 al., 2013) and packed-bed soil column systems, with the latter being mostly applied. In general,
98 although the comparison between these studies is complicated by the differences in experimental
99 settings and materials utilized (e.g. soil matrices, NPs compositions and coatings), a high mobility of
100 the QDs was observed at low ionic strength and neutral pH in unsaturated conditions representative
101 of natural subsurface systems (Usuyur et al., 2010) as well as in saturated granular matrices consisting
102 of either standardized porous media (e.g. quartz sand) or real soil samples (Torkzaban et al., 2010; Al-
103 Salim et al., 2011). However, retention of the QDs during column experiments was greatly enhanced
104 in presence of divalent cations, likely due to cation bridging between the negatively charged capping
105 groups (Quevedo & Tufenkij, 2012; Torkzaban et al., 2013), and when the collector surface presented
106 impurities or was coated with iron (Torkzaban et al., 2010). Wang et al., (2013) systematically studied
107 the effect of ionic strength, pH and NPs coating on the transport of QDs and reported enhanced
108 mobility at decreasing ionic strength and increasing pH as well as a diminished retention of the
109 carboxylated compared to the non-ionic coated NPs. These works agreed that QDs coating will
110 ultimately affect their behavior in the real terrestrial systems and that its interaction with the natural
111 components will determine the stability and environmental fate of the NPs. However, alteration of
112 the nanomaterials pristine state during the transport experiments was scarcely investigated and may
113 include ligand desorption, oxidation and aggregation/precipitation of the QDs, which have been

114 reported in aqueous systems as a consequence of irradiation and depending on solution chemistry
115 (Aldana et al., 2001; Zhang et al., 2008; Zhang et al., 2008b; Lead et al., 2018). In soil, Navarro et al.,
116 (2011) found evidences of degradation during leaching studies in presence of organic matter and
117 suggested that the stability of these chemicals over the long period is questionable whereas, more
118 recently, Faucher et al. (2018) reported dissolution and aggregation of the QDs in soil solutions.
119 However, the extent and kinetic of these phenomena remain unclear, especially regarding QDs
120 dissolution, which may cause the release and mobilization of novel potentially toxic species such as
121 Cd^{2+}, Se^{2-} and SeO_3^{2-}. Furthermore, such processes may be affected by QDs ageing and general
122 alteration of their pristine state. For instance, increased toxicity was reported on Zebra Fish and
123 bacteria as a consequence of QDs weathering (Mahendra et al., 2009; Wiecinski et al., 2013) whereas
124 Torkzaban et al. (2013) found a diminished release of deposited QDs from the soil with increasing
125 ageing time. However, to date most of the studies on QDs environmental fate were focused on
126 pristine as-produced nanomaterials, which physico-chemical properties may be representative of the
127 behavior occurring at manufacturing and processing sites but not upon release in the environment
128 (Lowry et al., 2012). In this context, Mitrano and Nowack (2017) recently stressed the need for novel
129 research focused on the transformation and ageing of nanoparticles, in order to better represent the
130 real conditions at which they are found in the ecosystem and allow a more precise and life-cycle
131 based assessment of these nanomaterials.
132 In this work we examined the mobility and stability of two QDs nanoparticles presenting nearly
133 identical nanocrystalline structure but different organic coating. A series of soil leaching experiments
134 were conducted to study the behavior of the two QDs in quartz sand, with regard to leached but also
135 deposited amounts, which have often been neglected in literature. The comparison between
136 fluorescence emission and mass spectrometric measurements allowed an estimation of NPs

137 transformation during the experiments whereas a further assessment of the NPs dissolution was
138 provided by ultrafiltration of the leached samples. A second set of experiments was devoted to
139 understanding the effect of NPs alteration and ageing on these processes. In particular, we
140 investigated the effect of I) increased Ca^{2+}-mediated homo-aggregation of the QDs in the spiking
141 solution and II) the ageing of the NPs in the column systems, i.e. their incubation in quartz sand for 15
142 days prior the experiments. The main aim of this study is to provide observation of QDs behavior in
143 simplified environmental systems, which can provide the basis for future works in more complex
144 matrices. These results will help the understanding of nanomaterials behavior and fate in soils, with
145 particular regard to small NPs such as QDs, as well as the effects of their transformation and ageing in
146 environmental systems.
147
148
149 2. Materials and Methods
150
151 2.1. Chemicals and Quantum Dots synthesis
152
153 The chemicals used for QDs nanocrystals and organic coating synthesis were purchased from Sigma
154 Aldrich (unless specified) and used without further purification: sulfur (99.9%), cadmium oxide
155 (99.9%), selenium (99.9%), anhydrous zinc acetate (99.9%), oleic acid (90%), trioctylphospine (90%), 1-
156 octadecene (90%), chloroform (99%), thioglycolic acid (99%), poly(maleic anhydride-alt-1-octadecene)
157 and ethanolamine (99%, Alfa Aesar). Concentrated nitric acid (65%) for samples acidification and
158 digestion and hydrogen peroxide (30%) were purchased from VWR whereas ultra-pure milli-Q water
159 (UPW) was produced in the laboratory with a Millipore purification system (Merck, Fontenay-sous-

160 Bois, France). The core-shell CdSe/ZnS QDs were synthesized in our group according to the single-step
161 protocol reported by Bae et al., (2008) with minor modifications, i.e. the use of zinc oxide instead of
162 zinc acetate as precursor. Purification of the QDs was achieved as following: first, the nanocrystals
163 were dissolved in chloroform and isolated by precipitation after centrifugation at 6000 rpm for 10 min
164 (5810 R centrifuge; Eppendorf Amburg, Germany). Then, the excess of reagents was removed with
165 consecutive steps of centrifugation (6000 rpm, 10 min) and filtration (PTFE 0.2 µm, Sigma Aldrich).
166 After the synthesis, different batches of QDs nanocrystals were functionalized with organic polymers,
167 in order to enhance their solubility in aqueous media. Two different coatings were selected based on
168 synthesis reproducibility and yield. Specifically, the relatively simple thioglycolic acid, consisting of a
169 short organic chain presenting both thiol and carboxylic acid functional groups (TGA, Zhu et al., 2014)
170 was compared to the more complex organic polymer poly(maleic anhydride-alt-1-octadecene)
171 (POAMA, Pellegrino et al., 2004). According to Faurier et al., (2017), the QDs are expected to have a
172 CdS gradient between the CdSe core and the ZnS shell whereas the yellowish color and fluorescence
173 emission in the green portion of the visible spectra indicated NPs diameter of 7 nm, with core size of
174 circa 3.4 nm. The final QDs stock solutions in ultrapure water and at pH 11 were stored at 4C in the
175 dark and a visual assessment of their homogeneity and limpidity was routinely performed with a
176 BTCP-20.MC compact transilluminator (Vilber Lourmat, Collegien, France).
177
178
179 2.2. Soil leaching experiments
180
181 IOTA high purity quartz sand from Unimin Corporation (Le Sueur, MN, US) was used as the porous
182 media for all the soil leaching experiments. Grain size observed with Scanning Electron Microscopy

183 coupled to Energy Dispersive X-Ray Analysis (SEM-EDX) ranged from 280 to 340 μm (n=20), with
184 average grain diameter of 300 μm. In order to remove metals and organic impurities from the quartz
185 sand, a cleaning protocol was performed similar to what reported by Wang et al., (2010). Briefly, the
186 sand was soaked in 10% HNO_3 placed in an ultrasonic bath (Ultrasonic Cleaner, VWR) at 60 Hz for 30
187 min and stirred every 5 min. The same procedure was repeated once with UPW, then once with 5%
188 H_2O_2 and eventually twice with UPW. The whole wash/rinse protocol was carried out three times and
189 the sand was eventually rinsed with 1 mM $Ca(NO_3)_2$ until pH equilibration, then rinsed with UPW and
190 oven dried at 65 C. The column apparatus consisted of custom-made 23 mL volume polycarbonate
191 columns (internal diameter 2.3 cm, length 4 cm) equipped with 25 mm polycarbonate filter holders
192 (Sartorius GhbH, Goettingen, Germany) sealed with polytetrafluoroethylene (PTFE) seal tape to
193 prevent leaking. Glass fiber filters (HA type; VWR) were placed at both extremities and approximately
194 23 g of quartz sand were added to each column with 0.5 cm increments in wet-packing conditions. A
195 background electrolyte, consisting of 1 mM $Ca(NO_3)_2$ solution at pH 7 was flushed in bottom-up mode
196 through the vertically oriented columns at a constant flow of 0.5 mL/min using a peristaltic pump
197 (Minipuls3; Gilson, Middleton, WI, USA). The resulting pore-water velocity of 4.5 m/day is
198 representative of typical coarse textured porous media and has been previously applied to study the
199 transport of NPs in saturated column systems (Torkzaban et al., 2013). At these conditions, the
200 porosity and pore volume (PV) were about 0.4 and 6.5 mL respectively, with PV residence time in the
201 column of 13 min. Each soil leaching experiment was performed in duplicate and the columns were
202 covered with aluminum foil to prevent exposure to light. The columns were first equilibrated with the
203 background electrolyte solution for at least 24 hrs (circa 100 PV) before introducing 0.5 mL of QDs
204 spiking solutions and 0.5 mL of a 120 mg/L Br^- tracer solution with the procedure reported by Navarro
205 et al. (2011). A scheme of the experimental set-up is provided in the supplementary info, fig. S1. 0.5

206 ml/min; 4.5 m/day). Spiking solution of the QDs in 1 mM $Ca(NO_3)_2$ and pH 7.0 were obtained from
207 dilutions of the stock solution for a concentration of 10.5 ± 0.1 μg/mL Cd. This corresponded to 8.5 ±
208 1.5×10^{13} particles/mL (14.1 ± 2.5 nM) based on a CdSe density of 5.82 g/cm^3 and assuming NPs
209 spherical shape with diameter of 3.4 nm. For experiments with altered (aggregated) QDs, spiking
210 solution was prepared in 100 mM $Ca(NO_3)_2$ solution, stored at room temperature in the dark for 4 hrs
211 and then ultrasonicated for 15 min before introduction. For ageing experiments the QDs spiking
212 solution was applied into the column, the peristaltic pumps were stopped, the tubing blocked with
213 clamps and the experiments re-started after 15 d of incubation. In each experiment, after
214 introduction of the QDs, 7 PV of background electrolyte were run through the column and 2 mL
215 eluent samples were collected into 5 mL polypropylene vials. This corresponded to a resolution of
216 circa 3 samples per PV. At the end of the experiments, the columns were first frozen at -18 °C
217 overnight and then the quartz sand was extracted and cut into thin sections of 0.3 to 0.5 mm thick.
218 The sections were transferred into 10 mL glass vials and freeze-dried with a Alpha 1-4 LD plus freeze
219 drier (Bioblock Scientific, Rungis Complexe, France) operating at approximately -56 °C and 0.035 mbar
220 for 48 hours.
221
222
223
224 2.3 Samples processing and analysis
225
226 In general, since fluorescence emission is peculiar of the QDs nanocrystals, at least with regard to the
227 pristine nanoparticles andFigures CdSe cores (Pereira et al., 2016), it was used for estimation of the
228 nanoparticle species during the experiments. Total Cd and Se were measured before and after

ultrafiltration (3 KDa) in order to assess total and dissolved metals concentrations, respectively. In detail, the 2 mL column eluent samples underwent fluorescence emission analysis for estimation of the QDs concentration and metal determination to assess the total Cd and Se contents. For fluorescence analysis, 0.5 mL was transferred into 5 mL polypropylene tubes and diluted with 3.5 mL of 1 mM $Ca(NO_3)_2$ at pH 7 then analyzed within 3 min from the collection to minimize alteration of the analytes (e.g. dissolution with consequent loss of fluorescence). For metal content analysis, 0.5 mL samples was transferred into 14 mL Falcon tubes, diluted up to 10 mL with UPW and acidified for a final 1% HNO_3 concentration. Additional 0.5 mL sample underwent ultrafiltration with 3 KDa regenerated cellulose centrifugal filters (Amicon 4-ultra, Merck), operated with centrifugation at 4000 rpm for 35 min. The filtrated samples were then diluted and acidified for Cd and Se analysis following a similar procedure than above. For time reasons, the ultrafiltration was carried twice during each experiment with sets of 9 samples each. The remaining amount was stored at 4°C in the dark. Extraction of the QDs from the lyophilized quartz sand sections was achieved with 15 min ultrasonication of 0.5 g samples in 4 mL of 50 mM NaCl solution at pH 10 at room temperature. Specifically, Na^+ was employed to enhance the extraction of the deposited QDs via cation exchange onto the sand surface whereas the high pH prevented dissolution and aggregation/precipitation of the QDs in solution (Torkzaban et al., 2013). Recovery of extraction of the QDs from the quartz sand were 78 ± 3 % and 85 ± 2 % for TGA-QDs and POAMA-QDs, respectively. Acid digestion was carried out for the analysis of metals in the solid samples as following: first, 0.5 g of each sample was transferred into 50 mL falcon tubes and 3 ml of concentrated acid (1:1; HNO_3:UPW) were added before undergoing ultrasonication for 30 min at room temperature. Then, 2 mL of H_2O_2 and 3 mL of UPW were added and the samples ultrasonicated again at the same conditions. Eventually, the samples were diluted 6 times with UPW for a final 2% HNO_3 concentration. The recovery for Cd and

252 Se extraction from the quartz sand was 96 ± 3 % and 92 ± 4 %, respectively. Fluorescence emission
253 analysis of both eluent and soil extracts samples were performed with a Horiba Scientific FluoroMax-4
254 spectrofluorimeter, with excitation wavelength set at 310 nm and emission spectra recorded in the
255 480-600 nm range. The measurements were repeated at least two times per samples and
256 quantitation was achieved with external calibration lines obtained from dilutions of the QDs stock
257 solutions at concentrations ranging from 1 to 500 μg/L Cd (at least 6 points). Limit of quantitation for
258 the QDs, based on Cd concentration, was 0.3 μg/L (equivalent to 2.1E+9 particles/mL). The metal
259 content in the samples was analysed with a sector field inductively coupled plasma mass
260 spectrometer (SF-ICP-MS, Element II, ThermoScientific, Bremen, Germany). Measurements of Se and
261 Cd were carried out in high and low resolution modes, respectively. Quantitation was achieved
262 analyzing standard solution at known concentrations of the elements ranging from 1 ng/L to 10 μg/L
263 (n=5) and Indium at the concentration of 1 μg/L was continuously introduced during each analysis as
264 internal standard. Limit of detection and quantitation were in the 100 ng/L and 10 ng/L ranges for Se
265 and Cd, respectively. The data were processed with uFreasi software (Tharaud et al., 2015). Analysis
266 of the metals digested from the quartz sand were done with an ICP-OES ICAP 6000 Series
267 (ThermoScientific) equipped with an ASX-520 autosampler (Cetac, Omaha, NE, USA). Bromide
268 tracer analysis were performed with a Dionex ICS 1100 ion chromatography system equipped
269 with AS DV autosampler (ThermoScientific).
270
271
272 3. Results and discussion
273 3.1. Mobility and Transformation of QDs
274

The synthesized NPs presented very similar CdSe/ZnS core-shell structures, with Zn/Cd ratio of 2.8 and 3.0, and Zn/Se ratio of 7.8 and 8.7, for TGA-QDs and POAMA-QDs, respectively. Furthermore, the QDs displayed similar fluorescence spectra in the green portion of the visible spectrum (500- 600 nm), with maximum yield at excitation wavelength of 310 nm and emission centered at 551 nm and 534 nm for TGA-QDs and POAMA-QDs, respectively (supplementary info, fig. S2). Thus, the main difference between the two NPs under investigation consisted in the ligand covalently attached to the surface, with TGA being a short organic chain and POAMA a more complex aromatic polymer (supplementary info, fig. S3 and S4). In this work, the fluorescence measurements were considered as indicative of a nanoparticles state, since the loss of emission is expected to correspond to a severe alteration of their core-shell structure (e.g. total dissolution). It must be noted that these could not necessarily discern between pristine and slightly altered nanomaterials (e.g. following partial dissolution of the ZnS shell). Fluorescence was compared with the ICP-MS measurements, which provided a quantitative assessment of the QDs metals but no information about their state (e.g. NPs or free ions). The mass balances for each experiment are provided in supplementary information (Table S5). Since Zn mass balances were generally >120% at the end of the experiments, Zn was not considered for further evaluation. Higher Zn concentrations may be due to background levels in the porous media or eluent solutions as well as incidental introduction during samples treatment. Thus, the results presented here are focused on Cd and Se analysis, which seemed not affected by Zn imbalances and presented recoveries generally > 90%.

297 The first aim of the present work was to study the QDs mobility during soil leaching experiments and
298 to provide an assessment of their behavior and transformation. Figure 1 shows the breakthrough
299 curves (BTC) obtained for POAMA-QDs (Fig. 1a) and TGA-QDs (Fig. 1b) in which NPs in the leachate
300 (fluorescence, black lines) are shown together with Cd (red) and Se (green). Similar to what was
301 reported by Al-Salim et al. (2011) during column studies in silt loam top-soil systems, the QDs were
302 eluted after 1 PV at the beginning of the experiments and displayed little or no significant difference
303 in the physical transport when compared to the conservative Br-tracer (supplementary info, fig. S6).
304 However, ICP-MS analysis revealed that different processes occurred during the transport due to
305 differences between the NPs in the capping ligand stability. Specifically, POAMA-QDs (fig. 1a) metals
306 BTCs were well correlated and displayed no significant difference with the measured fluorescence,
307 suggesting that Cd and Se were transported as clusters and that QDs leached from the columns in a
308 nanoparticulated form, at least with regard to the CdSe inner core liable for fluorescence emission.
309 The core integrity was further confirmed by the absence or low concentrations of Cd and Se after
310 samples ultrafiltration (Fig. 1a, light lines), which is selective for the QDs and generally for particles
311 larger than 3 KDa. Cd traces (in ultrafiltrates) were also measured immediately at the starting of the
312 experiment and likely belonged to endogenous Cd, which eluted from the column before QDs. In
313 contrast, TGA-QDs were slightly more retained in the column, with elution starting after 1.3 PV, and a
314 significant difference between NPs and metals BTC was observed (fig. 1b). Indeed, while QDs
315 concentrations were negligible, almost 40% of total Se and 0.5% of Cd were recovered in the leachate.
316 This indicates that QDs transformation occurred during the experiment, resulting in the release of
317 dissolved metal species, which transport was enhanced in comparison with the nanoparticulate
318 forms. Also, since Se is confined into the inner portion of the QDs core-shell structure, its large
319 concentration in the leachate necessarily implies at least a partial removal of both the ZnS shell and

320 organic coating outer layers. In general, such degradation is cause of concern for mobilization of
321 potentially toxic elements from NPs, including Cd(II), Se(-II), Se(IV) and several reactive oxygen species
322 (ROS) (Yaghini et al., 2014). In this context, the larger amount of Se in the leachate can be explained
323 assuming the formation of novel oxyanions Se species (such as SeO_3^{2-}), similar to those reported by
324 Navarro et al., (2011) during soil leaching studies, and considering the electrostatic repulsion with the
325 negatively charged quartz sand. Accordingly, Cd divalent cation retention is in agreement with its fast
326 sorption kinetic to soil. However, no Cd and only half of eluted Se were present in the samples after
327 ultrafiltration (fig. 1b, light lines). Since the low fluorescence measured in the non-filtered leachate
328 precluded the presence of large amounts of intact CdSe cores, the Se retention observed suggests the
329 formation of colloidal metal phases withheld in the 3 KDa membrane. Interestingly, colloidal Se
330 species (such as hydrogen selenide ion ,HSe^- and colloidal elemental selenium) were reported to
331 catalyze aerobic oxidation of thiols (Nuttal and Allen, 1984) and it could be expected that their
332 released after a first dissolution of the TGA-QDs, may have further enhanced the ligand
333 transformation, leading to the extensive degradation observed. In general, although the original
334 assumption was of non-favorable deposition conditions, with minimal retention due to the
335 electrostatic repulsion between NPs and quartz sand, both QDs displayed a strong retentive behavior
336 and leached fractions were 2.1% and 0.1% only of the POAMA-QDs and TGA-QDs initial amounts,
337 respectively. Torkzaban et al., (2013) reported deposition of 94% of the acrylic-capped CdTe QDs,
338 which is similar to the Cd and Se POAMA-QDs deposition in this study (~93%), suggesting that
339 enhanced NPs retention was due to the presence of divalent cations in solution (2 mM $CaCl_2$). In
340 detail, Ca^{2+}-mediated deposition can be explained with the compression of the electrical double layer
341 onto the NPs surface, which in turn determined a decreased repulsion between NPs and mineral
342 surface. Furthermore, enhanced deposition of the QDs could result from the formation of homo-

343 aggregates due to both the diminished mutual repulsion between NPs and the capacity of multivalent
344 cations to complex the NPs by bridging the negatively charged capping groups (Quevedo and Tufenkji,
345 2011; Torkzaban et al., 2013).
346
347 In fig. 2, soil profiles were plotted to show the retained QDs and metals distribution along the
348 columns. With regard to the POAMA-QDs (fig. 2a), although 77% of the deposited NPs was found in
349 the first 0.5 cm, gradually decreasing amounts in the further sections revealed that the QDs migrated
350 along the soil profile. Similarly, the larger fractions of Cd (71%) and Se (57%) were retained in the top
351 column with smaller concentrations detected in the further sections. The correlation between metals
352 and QDs distributions suggested that most of the NPs were intact during migration, confirming the
353 overall stability previously observed in the leachate. Despite this the NPs quantified on the basis of
354 fluorescence emission, which is indicative of pristine structures and/or CdSe cores (Pereira et al.,
355 2016) accounted for 76% of the initial amount, showing that also a portion of the POAMA-QDs were
356 altered after or during deposition. This observation is further supported by the minor differences
357 between Cd and Se concentrations in the column segments, with the latter moving deeper along the
358 profile. As expected from the analysis of the leachate, such phenomena had a larger extent in TGA-
359 QDs amended column (fig. 2b). Indeed, although the quasi totality of Cd and 55% of Se were
360 recovered in the quartz sand, according with the amounts measured in the eluent, only 25.9% of
361 these corresponded to pristine QDs. Furthermore, while Cd and Se had a distribution similar to that of
362 POAMA-QDs, with >65% of the metals in the top-column and the rest distributed in the further
363 sections, the NPs displayed no migration and were entirely (> 95%) accumulated in the first 0.5 cm.
364 The concentration of Se and QDs in this section were similar and within the measured error,
365 indicating that Se was retained in the top column as NPs and that transport occurred only for the

366 species resulting from NPs degradation. Thus, it can be assumed that in addition to exposing the core-
367 shell nanocrystals to the outer environment, with consequent dissolution phenomena, the ligand
368 removal also caused the immobilization of the QDs onto the porous media due to the loss of surface
369 coatings negative charges and non-favorable deposition conditions. It must be noted that the
370 instability of thiol-capped QDs, similar to those in this work, was investigated by previous studies in
371 aqueous media, which reported a pH-dependent aggregation and capping desorption of the NPs as
372 well as light-mediated oxidation with consequent precipitation of the nanocrystals (Aldana et al.,
373 2001; Zhang et al., 2008b). However, the same works highlighted the relative stability of QDs
374 (homogeneous dispersion and no precipitation) at the experimental conditions we applied (neutral
375 pH, no light exposure) suggesting that degradation during the leaching experiments was enhanced by
376 their interaction with the quartz sand matrix. Nonetheless, similar transformation phenomena were
377 often neglected during soil transport studies, given the assumption that QDs were stable in soil
378 matrices and during the relatively short duration of typical column experiments (usually 1-3 hrs) (e.g.
379 Wang et al., 2013), and evidences of QDs degradation were only reported after long-term exposure of
380 NPs in soil systems (Navarro et al., 2011). Rather, we observed that a fast ligand desorption may occur
381 in soil with consequent transformation of the nanomaterials in the short-term. In this context, similar
382 processes may hinder both the qualitative (speciation) and quantitative (deposition, attachment
383 efficiency) assessment of QDs fate. For instance, in the case of TGA-QDs in this study the analysis of
384 QDs fluorescence only may lead to an overestimation of deposited amounts, whereas mass
385 spectrometric measurements alone would result in the overestimation of the eluted QDs.
386
387
388 3.2 Effect of Ageing and Alteration of the QDs

389

390 Once released in the environment, NPs will undergo modification of their state and properties due to
391 the interactions with the natural components and ageing in the natural media (Mitrano and Novak,
392 2017). Thus, a second set of soil leaching studies was carried out to investigate the effect that
393 alteration of the pristine QDs may have on their behavior during their transport in soil.

394

395

396 In the first ageing experiment, POAMA-QDs spiking solution was prepared at a larger concentration of
397 Ca^{2+} and incubated in the dark for a few hours before being introduced in the column. As shown in fig.
398 3a, this resulted in a higher QDs sorption onto quartz sand, and their complete retention in the
399 column, i.e. no fluorescence measured in the leachate. A fraction of Cd and Se (0.5+/-0.1 % and 6.9+/-
400 2.4 %; respectively) eluted at the beginning of the experiment with leaching profiles similar to those
401 of the pristine QDs (Fig. 1a). However, no significant difference was observed with the concentrations
402 found after ultrafiltration of the samples, suggesting that these were free metal species formed either
403 in the preparation and ageing of the spiking solution or during NPs transport in the column.
404 Homo- and hetero-aggregation of nanomaterials are important processes driving their environmental
405 fate and effects (Lead et al., 2018) and their characterization (e.g. kinetics of aggregation,
406 determination of attachment efficiency) is increasingly being used for predicting NPs behavior and
407 transport models (Geitner et al., 2017). Increasing ionic strength of multivalent cations in solution is
408 known to cause increasing hydrodynamic diameters and reduced electrophoretic mobility of QDs
409 (Wang et al., 2013; Quevedo and Tufenkji, 2011). For instance, Quevedo and Tufenkji (2011) reported
410 up to 15-fold increase of CdSe QDs diameter (assessed by transmission electron microscopy, TEM) at
411 Ca^{2+} concentrations similar to those applied in the present study (2,5 mM). In this case, the

412 hydrodynamic diameter of QDs, measured by dynamic light scattering (DLS) was circa 550 nm and
413 resulted in enhanced retention and one order of magnitude increase in the attachment efficiency.
414 Although such measurements were not performed here, recent studies by some of the authors of this
415 work showed aggregation of POAMA-QDs in aqueous suspensions and soil solutions (Faucher et al.,
416 2018). Thus, it can be assumed that homo-aggregation of the NPs prior introduction in the columns
417 imposed a reduced transport due to the larger size and smaller charge density of QDs. This also
418 resulted in a decreased mobility along the soil profile (fig. 2c), with 95% of the retained NPs
419 accumulated in the top-columns together with the largest fractions of Cd and Se. The metals were
420 recovered to a larger extent, specifically 94% and 97% for Cd and Se, respectively (SI, table S4).
421 Furthermore, in the quartz sand, 80% or the metals were found in NPs form, indicating the relative
422 stability of the altered NPs, likely due to the decreasing of the surface to volume ratio in the
423 aggregates, i.e. a smaller surface exposed to the outer environment. Based on these results, it can be
424 expected that aggregation will determine an even more limited mobility and higher persistency of
425 QDs in terrestrial systems. However, it must be noted that the present work investigated the effect of
426 homo-aggregation processes, which may only be representative of specific environmental scenarios
427 where the presence of high concentrations are expected (e.g. disposal of consumer products, hot-
428 spots of contaminations) and that future works will need to clarify the effect of hetero-aggregation
429 phenomena (e.g. interaction with organic matter), which are generally considered more relevant after
430 dispersion of engineered nanomaterials in real ecosystems.
431 In the final set of experiments, NPs were aged in contact with the quartz sand before leaching in order
432 to determine changes in their behaviour and mobility over time. Thus, the experiments were carried
433 out at the same experimental conditions as previously (see section 3.1), but elution started 15 days
434 after the introduction of QDs in the columns. The incubation time of 15 days was chosen in order to

435 represent short to medium ageing periods and was previously applied in environmental fate studies
436 (Navarro et al., 2011). In general, ageing resulted in a reduced NPs transport in comparison to the
437 non-aged experiments, with neither of the two QDs types leaching from the columns (fig.3b and 3c,
438 black lines), and with retained fractions being almost totally (98%) accumulated in the first section of
439 the soil profile (fig. 2d and 2e, fluorescence bars). This behavior can be explained by an enhanced
440 time-dependent NPs sorption to the quartz sand, as well as the consequence of homo-aggregation
441 induced by the presence of a high NPs concentration in the top column for a relatively long period.
442 Navarro et al., (2011) reported increased mobility of thiol coated CdSe QDs after ageing in soil
443 matrices due to the presence of organic matter in the system (i.e. ethylenediaminetetraacetic acid in
444 the eluent and native organic acids in the soil). Furthermore, the authors found evidences of NPs
445 degradation over time and suggested that organic material acted as chelating agent for the metals
446 species originated from the QDs. In this study, both QDs were transformed to a large extent but in the
447 absence of organic matter the etching of the pristine structures (e.g. transformation/desorption of
448 the capping ligands) likely contributed at enhancing their deposition onto the sand. Indeed, the
449 overall recovery from the system was only 22 +/- 5 % of the original POAMA-QDs (fig. 3b) and 8 +/- 2
450 % for TGA-QDs. Notably, while a larger degradation of the latter was expected due to its lower
451 stability (see section 3.1), severe transformation were also observed for POAMA-QDs, which instead
452 remained almost intact in the non-aged experiments. Accordingly, the metal species resulting from
453 NPs dissolution were more abundant in TGA-QDs leachate, and predominantly consisted of Se, due to
454 preferential Cd sorption to the sand. As shown in fig. 3b and 3c, the ageing also caused significant
455 changes leaching profiles of the metals, which eluted immediately at the beginning of the
456 experiments, probably because of Cd and Se species migration in the saturated system during the
457 incubation time. Interestingly, the overall larger degradation observed in the aged columns did not

458 result in a faster transport of metals in the liquid phase. Indeed, Se amounts in the leachate were
459 lower than those found in the non-aged experiments and specifically 2.9 +/-0.6 % and 13.6 +/- 5.2 %
460 for POAMA-QDs (fig. 3b) and TGA-QDs (fig. 3c), respectively. However, similar concentrations were
461 found after ultrafiltration, specifically 2.4 +/- 0.1 for POAMA-QDs and 11.1 +/- 4.5, for TGA-QDs,
462 suggesting that only free metal ions (e.g. SeO_3^{2-}) were transported and that the metal colloids
463 previously observed in the TGA-QDs non-aged column leachate (see fig. 1b) were deposited onto the
464 quartz sand. Consequently, the amount of Se retained in the columns increased significantly from 54%
465 of the non-aged experiments to 79% in aged TGA-QDs experiments. Analysis of the soil column
466 profiles (fig. 2d and 2e) confirmed that Cd and Se did not consistently move as a cluster in the quartz
467 sand confirming the disruption of the NPs form. Specifically, in both studies more than 90% of Cd was
468 accumulated in the first 0.5 cm whereas Se was detected throughout the soil column profiles, with
469 larger migration in TGA-QDs columns where >50% of Se migrated from the introduction spot to
470 further segments. Nonetheless, fluorescence emission recorded in the top column sections extracts
471 showed the presence of potentially intact CdSe QDs cores deposited. However, analysis of the spectra
472 revealed that an 11 nm blue-shift was present in the emission maximum of the TGA-QDs whereas
473 POAMA-QDs spectra had a 4 nm shift to the right (supplementary info, fig. S7 and S8). Interestingly,
474 similar red-shift was also recorded for QDs recovered from the columns amended with altered spiking
475 solution, i.e. where homo-aggregation was enhanced. Since QDs emission is correlated to their size,
476 with emission wavelengths decreasing with the NPs diameters, these results suggest that the CdSe
477 cores of TGA-QDs were partially altered and became smaller with ageing. On the contrary, deposited
478 POAMA-QDs cores were likely intact also due to aggregation phenomena that enhanced the sorption
479 onto the sand and prevented dissolution of the structure. Eventually, the results of the ageing
480 experiments showed that QDs will undergo profound alteration in the soil over time independently of

481 their synthetic route (i.e. the organic coating), but that the capping ligand will still determine the
482 kinetic at which these transformations will occur.
483
484 4. Conclusions
485
486 The transport of core-shell CdSe/ZnS QDs in quartz sand appeared to be limited at all conditions
487 tested: pristine, altered and aged NPs. However, it must be noted that the soil column systems
488 presented here were necessarily simplistic in comparison to real environmental systems, with regard
489 to porous media and eluent compositions. These factors will play a major role in determining NPs fate
490 in soils (Geitner et al., 2020) and experiments employing more complex matrices (e.g. in the presence
491 of minerals and organic matter) are currently being performed in our team. The results presented
492 suggest that QDs will be accumulated in surface soils upon release in the environment but dissolution
493 occurring due to the alteration of the pristine structures (i.e. capping ligand desorption) will result in
494 the formation of novel potentially toxic metal species, which mobility was enhanced in our
495 experiments in comparison with intact NPs. Thus, the stability of the organic coatings-NPs complexes
496 will be as important as their physico-chemical properties in dictating the eventual fate of QDs in soil
497 matrices, with regard to both their speciation and partitioning. In particular, small capping ligands
498 used in this study (e.g. thioglycolic acid, TGA) displayed faster desorption rates from the NPs surface,
499 resulting in the immobilization of the nanocrystals onto the sand. The organic coating removal likely
500 enhanced the exposure of ZnS shells and subsequently CdSe cores to the outer environment, resulting
501 in a larger degradation of the NPs. On the contrary, the stability conferred by larger organic coatings,
502 as the poly(maleic anhydride-alt-1-octadecene) (POAMA), will likely determine higher transport and
503 accumulation of the pristine QDs. Although alteration of the NPs manufactured state, such as homo-

504 aggregation, may prevent degradation and enhance their persistency, we observed severe NPs
505 transformation over time independently of their surface ligand. It must be noted that although the
506 characterization of as-produced NPs is fundamental for the understanding of their environmental
507 behavior, most nanomaterials are currently being incorporated in a variety of matrices, in the case of
508 QDs electronics and optics. Hence, future works will need to investigate the release of these
509 nanomaterials in the presence of (embedded) matrices in order to represent more realistic
510 release/mobility pathways and contamination scenarios (Nowack et al., 2016).
511 The results presented here suggest that the stability of the QDs in soils is questionable during both
512 the short- and long-term periods and that transformation phenomena will eventually determine the
513 removal of these nanomaterials from the soil compartments. Furthermore, degradation phenomena
514 may hinder a proper estimation and assessment of the QDs during transport and fate experiments,
515 and future works will need to address such issues. In this context, the use of multiple techniques has
516 been often recommended for the NPs characterization in environmental media in order to gather
517 information about their state (e.g. pristine, aggregated, dissolved). In this work, the comparison of
518 mass spectrometry and fluorescence analysis as well as the use of ultrafiltration proved to be valuable
519 tools in discerning the NPs forms among the metal species detected. Similar strategies were recently
520 applied by our team to determine quantum dots at low concentrations and in complex biological and
521 environmental matrices (Supiandi et al., 2019; 2020). Nonetheless, future works will need to provide
522 more qualitative information about the QDs speciation and to describe the occurrence of the
523 degradation products in real soil media and their interaction with natural components.
524
525
526

Acwnoledgements

The present study was funded by the Agence Nationale de la Recherche (ANR), France, project QUADOS: ANR-CE01-0013. The authors would like to acknowledge the support by IPGP multidisciplinary program PARI and by Region île-de-France SESAME Grant no. 12015908. The authors want to thank the Water Biogeochemistry team at the Institut de Physique du Globe in Paris for the active collaboration and particularly Mickael Tharaud and Dr. Morgane Desmau for the help during method development and samples analysis.

References

Al-Salim N., Barraclough E., Burgess E., Clothier B., Deurer M., Green S., Malone L., Weir G. **2011**. Quantum Dot transport in soil, plants and insects. *Sci Total Environ* 409. 3237-3248.

Aldana J., Wang Y. A., Peng X. **2001**. Photochemical instability of CdSe nanocrystals coated by hydrophilic thiols. *J Am Chem Soc* 123, 8844-8850.

Alivisatos A. P. **2004**. The use of nanocrystals in biological detection. *Nat Biotechnol* 22 (1), 47-52.

Anikeeva P. O., Halpert J. E., Bawendi M. G., Bulovic V. **2009**. Quantum Dot light-emitting devices with electroluminescence tunable over the entire visible spectrum. *Nano Lett* 9 (7), 2532-2536.

549 Bae W. K., Char K. Hur H., Lee S. **2008**. Single-step synthesis of quantum dots with chemical
550 composition gradients. *Chem Mater* 20, 531-539.

551

552 Bera D., Qian L., Tseng T., Holloway P. H. 2010. Quantum dots and their multimodal application: a
553 review. Materials 3, 2260-2345. doi:10.3390/ma3042260

554

555 Bruchez M. Jr., Moronne M., Gin P., Weiss S., Alivisatos A. P. **1998**. Semiconductor nanocrystals as
556 fluorescent biological labels. *Science* 281(5385), 2013-2016.

557

558 Cornelis G., Hund-Rinke K., Kuhlbush T., Van Den Brink N., Nickel C. **2014**. Fate and bioavailability of
559 Engineered nanomaterials in soils: a review. *Crit Rev Environ Sci Technol* 44, 2720-2764. DOI:
560 10.1080/10643389.2013.829767.

561

562 Dabbousi B. O., Rodriguez-Viejo J.,Mikulec F. V., Heine J. R., Mattoussi H.,Ober R., Jensen K.
563 F.,Bawendi M. G. **1997**. CdSe/ZnS core-shell Quantum Dots: synthesis and characterization of a size
564 series of highly luminescentnanocrystallites. *J Phys Chem B* 101 (46) 9463-9475.

565

566 Dunphy G. K. A., Taylor M. R., Banfield J. F. **2006**. Environmental risk of nanotechnology: national
567 nanotechnology initiative funding, 2000-2004. *Environ Sci Technol* 40 (5), 1401-1407.

568

569 Faucher S., Charron G., Lützen E., Le Coustumer P., SchaumLöffel D., Sivry Y., Lespes G. **2018**.
570 Characterization of polymer-coated CdSe/ZnS quantum dots and investigation of their behaviour in

soil solution at relevant concentration by asymmetric flow field-flow fractionation - multi angle light scattering – inductively coupled plasma - mass spectrometry. *Anal Chim Acta* 1028, 104-112.

Geitner N. K., O'Brien N., Turner A., Cummins E. J., Wiesner M. 2017. Measuring Nanoparticle Attachment Efficiency in Complex System. Environ Sci Technol 51(22). DOI: 10.1021/acs.est.7b04612

Geitner N. K., Hendren C. O., Cornelis G., Kaegi R., Lead J. R., Lowry G., Lynch I., Nowack B., Petersen E., Bernhardt E., Brown S., Chen W., de Garidel-Thoron G., Hanson J., Harper S., Jones K., Turner A., Liu J.,Unrine J., Vance M., White J. C., Wiesner M. 2020. Harmonizing Across Environmental Nanomaterial Testing Media for Increased Comparability of Nanomaterial Datasets Environ Sci-Nano 7, 13-36. DOI: 10.1039/C9EN00448C

Hardman R. **2006**. A toxicologic review of Quantum Dots: toxicity depends on physicochemical and environmental factors. *Environ Health Perspect* 114 (2), 165-172.

Kamat P. V. **2008**. Quantum Dot solar cells. Semiconductor nanocrystals as light harvesters. *J Phys Chem C* 112, 18737-18753.

Kalita H., Lekshmi S., Baghini M. S., Aslam M. **2016**. Graphene Quantum Dots Soil Moisture Sensor. *Chemical* 233, 582-590.

592 Karakoti A. S., Shukla R., Shanker R., Singh S. 2015. Surface functionalization of quantum dots for
593 biological applications. Adv Colloid Interface Sci 15, 28-45. doi.org/10.1016/j.cis.2014.11.004
594
595 Khare S. and Kumari A. **2017**. Adverse effect of CdTe quantum dots on the cell membrane of Bacillus
596 subtilis: insight from microscopy. *J Nanoso* 12, 19-26.
597
598 Lead J. R., Batley G. E., Alvarez P. J. J., Croteau M., Handy R. D. , McLaughlin M. J., Judy J. D., Schirmerh
599 K. 2018. Nanomaterials in the environment: behavior, fate, bioavailability, and effects—an updated
600 review. Environ Tox Chem 37 (8), 2029-2063. DOI: 10.1002/etc.4147
601
602 Lowry G. V., Gregory K. B., Apte S. C., Lead J. R. **2012**. Transformations of nanomaterials in the
603 environment. *Environ Sci Technol* 46, 6893-6899.
604
605 Mahendra S., Zhu H., Colvin V. L., Alvarez P. J. **2009**. Quantum Dots weathering results in microbial
606 toxicity. *Environ Sci Technol* 42 (24), 9424-9430.
607
608 Mitrano D. M. and Nowack B. **2017**. The need for a life-cycle based aging paradigm for nanomaterials:
609 importance of real-world test systems to identify realistic particle transformation. *Nanotechnology* 28
610 (7).
611
612 Navarro D. A., Banerjee S., Watson D. F., Aga D. S. **2011**. Differences in soil mobility and degradability
613 between water-dispersible CdSe and CdSe/ZnS Quantum Dots. *Environ Sci Technol* 45, 6343-6349.

Nowack B., Boldrin A., Caballero A., Hansen S. F. , Gottschalk F., Heggelund L., Hennig M., Mackevica A., Maes H., Navratilova J., Neubauer N., Peters R., Rose J., Schaffer A., Scifo L., van Leeuwen S., von der Kammer F., Wohlleben W., Wyrwoll A., Hristozov D. 2016. Meeting the Needs for Released Nanomaterials Required for Further Testing□The SUN Approach. Environ Sci Technol 50, 2747−2753. DOI: 10.1021/acs.est.5b04472

Nuttal K. L. and Allen F. S., 1984. Hydrogen selenide ion and colloidal selenium in the catalytic oxidation of thiols. Inor Chim Acta 93-2, 85-88. doi.org/10.1016/S0020-1693(00)87892-5

Oomen A. G.,□, Steinhäuser K. G., Bleeker E. A. J., van Broekhuizen F., Sips A., Dekkers S, Wijnhoven S. W. P., Sayre P. G. 2018. Risk assessment frameworks for nanomaterials: Scope, link to regulations, applicability, and outline for future directions in view of needed increase in efficiency. Nanoimpact 9, 1-13. doi.org/10.1016/j.impact.2017.09.001

Owen R. and Handy R. **2007**. Formulating the problems for environmental risk assessment of nanomaterials. *Environ Sci Technol* 41 (16), 307-309.

Pellegrino T., Manna L., Kudera S., Liedl T., Koktysh D., Rogach A. L., Keller S., Radler J., Natile G., Parak W. J. **2004**. Hydrophobic nanocrystals coated with an amphiphilic polymer shell: a general route to water soluble nanocrystals. *Nano Lett* 4, 703-707. doi:10.1021/nl035172j.

637 Pereira M. G. C., E.S.Leite., E. S., Pereira G. A. L., Fontes A., Santos B. S. 2016. Nanocolloids: A Meeting
638 Point for Scientists and Technologists, chapter 4, 131-158. doi.org/10.1016/B978-0-12-801578-
639 0.00004-7
640
641 Quevedo I. R. and Tufenkij N. **2009**. Influence of solution chemistry on deposition and detachment
642 kinetics of a CdTe Quantum Dot examined using a Quartz Crystal Microbalance. *Environ Sci Technol* 43
643 (9), 3176-3182. DOI: 10.1021/es803388u.
644
645 Quevedo I. R. and Tufenkij N. **2012**. Mobility of functionalized Quantum Dots and model polystyrene
646 nanoparticle in saturated quartz sand and loamy sand. *Environ Sci Technol* 46, 4449-4457. DOI:
647 10.1021/es2045458
648
649 Quevedo I. R., Olsson A. L. J., Tufenkij N. **2013**. Deposition kinetics of Quantum Dots and polystyrene
650 latex nanoparticles onto alumina: role of water chemistry and particle coating. *Environ Sci Technol* 47
651 (5), 2212-2220. DOI: 10.1021/es303392v.
652
653 Roco M. C. **2011**. The long view of nanotechnology development: the National Nanotechnology
654 Initiative at 10 years. *J Nanop Res* 13 (2), 427 – 445.
655
656 Supiandi N. I., Charron G., Tharaud M., Cordier L., Guigner J.-M., Benedetti M. F., Sivry Y. 2019.
657 Isotopically labeled nanoparticles at relevant concentrations: how low can we go? The case of
658 CdSe/ZnS QDs in surface waters. Environ Sci Technol. Do: 10.1021/acs.est8b04096

659

660 Supiandi N. I., Charron G., Tharaud M., Benedetti M. F., Sivry Y. 2020. Tracing multi-isotopically
661 labeled CdSe/ZnS quantum dots in biological media. Sci Rep 10, 2886. Doi.org/10.1038/s41598-020-
662 59206-w

663

664 Tharaud M., Gardoll S., Khelifi O., Benedetti M. F., Sivry Y. **2015**. UFREASI: User friendly elemental
665 data processing. A free and easy-to-use tool for elemental data treatment. *J Microc*.
666 10.1016/j.microc.2015.01.011

667

668 Torkzaban S., Kim Y., Mulvihill M., Wan J., Tokunaga T. K. **2010**. Transport and deposition of
669 functionalized CdTe nanoparticles in saturated porous media. *J Contam Hydrol* 118, 208-217.

670

671 Torkzaban S., Bradford S. A., Wan J., Tokunaga T., Masoudih A. **2013**. Release of Quantum Dot
672 nanoparticles in porous media: role of cation exchange and aging time. *Environ Sci Technol* 47. 11528-
673 11536.

674

675 U.S. EPA. EPA Nanotechnology White Paper. http://www.epa.gov/osainter/pdfs/nanotech/epa-
676 nanotechnology-whitepaper-0207.pdf.

677

678 Usuyur B., Darnault C. J. G., Snee P. T., Koken E., Jacobson A. R., Wells R. R. **2010**. Coupled effects of
679 solution chemistry and hydrodynamics on the mobility and transport of Quantum Dot nanomaterials
680 in the vadose zone. *J Contam Hydrol* 118. 184-198.

681

682 Wang Y., Li Y., Kim H., Walker S. L., Abriola L. M., Pennell K. D. **2010**. Transport and retention of
683 fullerene nanoparticles in natural soils. *J Environ Qual* 39. 1925-1933.
684
685 Wang Y., Zhu H., Becker M. D., Englehart J., Abriola L. M., Colvin V. L., Pennell K. D. **2013**. Effect of
686 surface coating composition on Quantum Dot mobility in porous media. *J Nanopart Res* 15. 1805. DOI:
687 10.1007/s11051-013-1805-0.
688
689 Wiecinski P. N., Metz K. M., Heiden T. C. K., Louis K., Mangham A. N., Hamers R. J., Heideman W.,
690 Peterson R. E., Pedersen J. A. **2013**. Toxicity of oxidatively degraded Quantum Dots. *Environ Sci*
691 *Technol* 47. 9132-9139.
692
693 Xiao Y., Ho K. T., Burgess R. M., Cashman M. **2016**. Aggregation, sedimentation Dissolution and
694 Bioavailability of Quantum Dots in estuarine systems. *Environ Sci Technol* 51 (3), 1357-1363. DOI:
695 10.2021/acs.est.6b04475.
696
697 Yaghini E., Pirker K. F., Kay C. W., Seifalian A. M., Mac Robert A. J. 2014. Quantification of reactive
698 oxygen species generation by photoexcitation of PEGylated quantum dots. Small. 10(24), 5106-5115.
699 doi: 10.1002/smll.201401209
700
701 Zhang Y., Chen Y., Westerhoff P., Crittenden J. C. **2008**. Stability and removal of water soluble
702 Quantum Dots in water. *Environ Sci Technol* 42. 321-325.
703

704 Zhang Y., Mi L., Wang P., Ma J., Chen J. **2008b**. pH-dependent aggregation and photoluminescence
705 behavior of thiol-capped CdTe Quantum Dots in aqueous solutions. *J Lumin* 128. 1948-1951.
706
707 Zhu H., Hu M. Z., Shao L., Yu K. Dabestani, R. Zaman, M.B. Liao, S. **2014**. Synthesis and Optical
708 Properties of Thiol Functionalized CdSe/ZnS (Core/Shell) Quantum Dots by Ligand Exchange. *J*
709 *Nanomater* ID e324972. doi:10.1155/2014/324972.
710

Figure captions

Manuscript Number: CHEM 69321
Title: Mobility and Transformation of CdSe/ZnS Quantum Dots in Soil: Role of the Capping Ligands and Ageing Effect

Figure 1

Figure 1. a) POAMA QDs breakthrough curves (BTC) of Se (green), Cd (red) and fluorescence (black) reported as fractions (%) of the initial amount introduced in the columns. The darker and lighter lines represent the total fraction eluted before and after ultrafiltration, respectively. b), BTC obtained for TGA-QDs. Due to the large gap between Cd and Se concentrations, Se values refer to Y axis on the right.

Figure 2

Figure 2. Soil column profiles obtained from analysis of the quartz sand after the leaching experiments. On top: a) POAMA-QDs, b) TGA-QDs. Bottom: c) aggregated POAMA-QDs solution, d) aged POAMA-QDs and e) aged TGA-QDs. Cd, Se, and NPs (fluorescence) are expressed as fraction of the initial amounts and each bar graph represent the percentage found in different sections of the columns.

Figure 3

Figure 3. Breakthrough curves of the QDs during ageing experiments. a) altered POAMA-QDs b) aged POAMA-QDs and c) aged TGA-QDs. The darker and lighter lines for Se (green) and Cd (red) represent the fraction eluted (%) before and after ultrafiltration, respectively. No fluorescence (black lines) was observed in any of the samples.

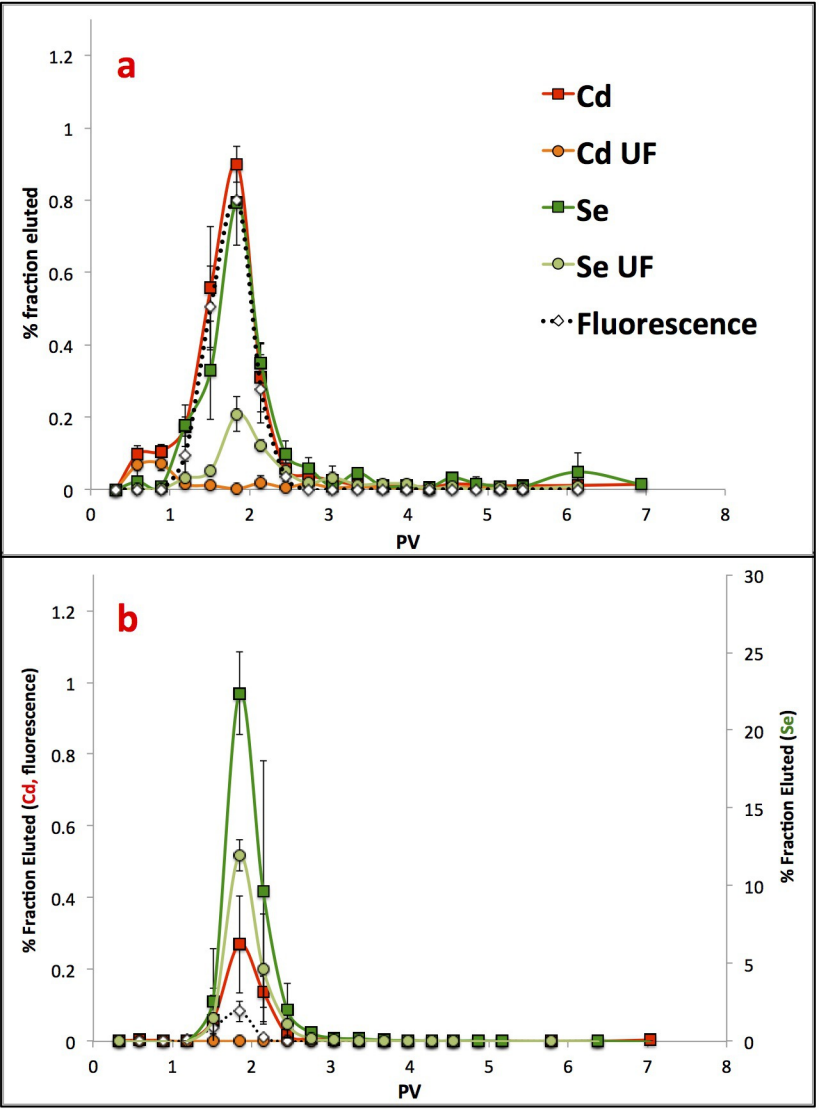
a
Cd
Cd UF
Se
Se UF
Fluorescence
% fraction eluted
PV
b
% Fraction Eluted (Cd, fluorescence)
% Fraction Eluted (Se)
PV

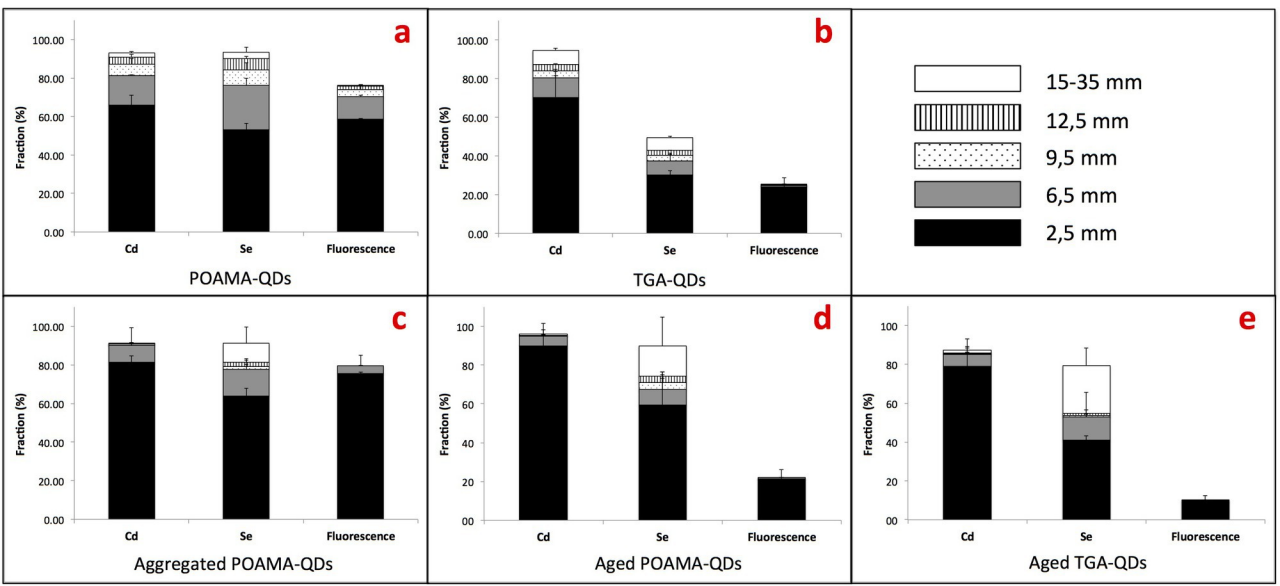
a
b
c
d
e
Fraction (%)
100.00
80.00
60.00
40.00
20.00
0.00
Cd
Se
Fluorescence
POAMA-QDs
TGA-QDs
Aggregated POAMA-QDs
Aged POAMA-QDs
Aged TGA-QDs
15-35 mm
12,5 mm
9,5 mm
6,5 mm
2,5 mm

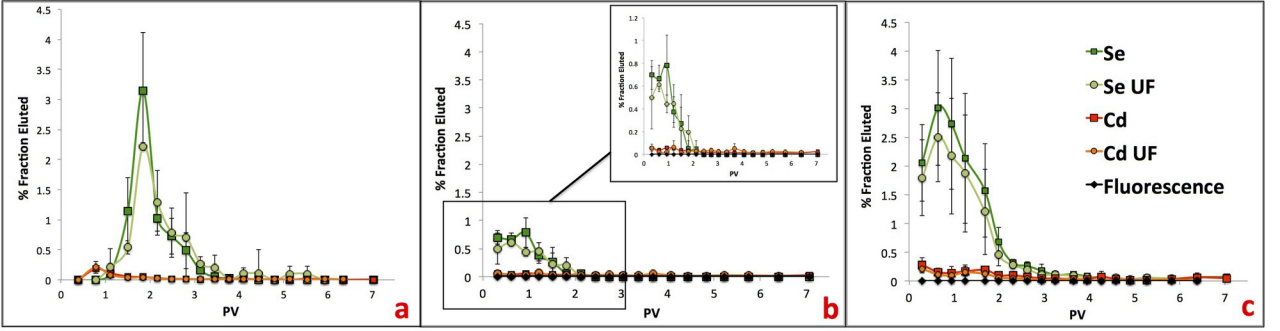
% Fraction Eluted
PV
a
b
c
Se
Se UF
Cd
Cd UF
Fluorescence

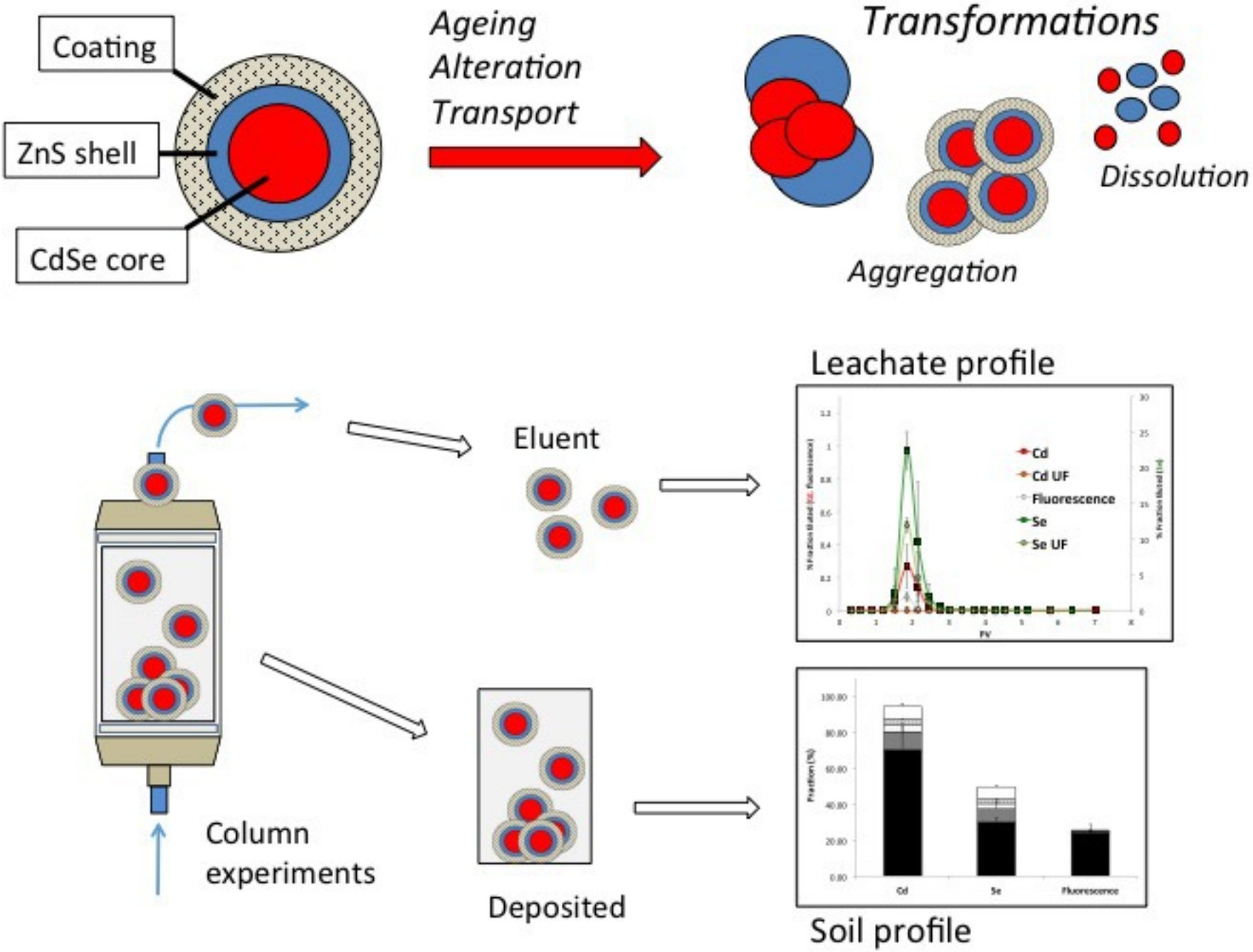
Coating
ZnS shell
CdSe core
Ageing
Alteration
Transport
Transformations
Dissolution
Aggregation
Leachate profile
Eluent
Cd
Cd UF
Fluorescence
Se
Se UF
PV
Column
experiments
Deposited
Cd
Se
Fluorescence
Soil profile